DOI: 10.1002/ejic.200900244

Organometallic Osmium(II) and Ruthenium(II) Biphenyl Sandwich Complexes: X-ray Crystal Structures and ^{187}Os NMR Spectroscopic Studies in Solution

Jennifer C. Gray,[a] Alain Pagelot,[b] Anna Collins,[a] Francesca P. A. Fabbiani,[a] Simon Parsons,[a] and Peter J. Sadler*[c]

Dedicated to Professor Jan Reedijk on the occasion of his 65th birthday

Keywords: Osmium / Ruthenium / Sandwich complexes / Arenes / NMR spectroscopy / Structure elucidation

We report the synthesis of the ruthenium(II) and osmium(II) organometallic sandwich complexes [Ru(η^6-bip)$_2$](OTf)$_2$ (**1**) and [Os(η^6-bip)$_2$](OTf)$_2$ (**2**) containing biphenyl (bip) as the arene ligand, and the X-ray crystal structures of **1**·MeOH and **2**. The unit cell of the osmium complex contains molecules in which the unbound phenyl ring of the biphenyl ligands exists in both staggered and eclipsed configurations, whereas for the ruthenium complex the rings are only eclipsed. Both crystal structures possess CH/π and π–π stacking interactions. ^{187}Os (nuclear spin 1/2, natural abundance of 1.64 %) has a very low gyromagnetic ratio and is one of the most insensitive nuclei in the periodic table. We show that inverse NMR spectroscopic detection by the use of ^{1}H/^{187}Os heteronuclear multiple bond correlation (HMBC) spectroscopy allows the ready observation of the ^{187}Os resonance of complex **2** via couplings to arene ring protons.

Introduction

Bioorganometallic chemistry is a rapidly developing field with opportunities especially for the design of novel therapeutic agents.[1–3] We have concentrated on the design of ruthenium(II) and osmium(II) arene half-sandwich complexes as anticancer agents, some of which are as cytotoxic to cancer cells as the clinical drugs cisplatin and carboplatin but not cross-resistant.[4,5] We have also explored the biological activity of arene sandwich complexes, for example containing the sweetener aspartame as a π-bonded ligand.[6]

In the present study we have investigated the synthesis and solid-state structures of ruthenium(II) and osmium(II) complexes [Ru(η^6-bip)$_2$](OTf)$_2$ (**1**) and [Os(η^6-bip)$_2$](OTf)$_2$ (**2**) containing biphenyl (bip) as the arene ligand and have discovered interesting subtle difference between their solid-state packing. We have explored the detection of ^{187}Os NMR signals from the sandwich complex **2** in solution. ^{187}Os is a spin-1/2 nucleus rendering it more favourable for NMR spectroscopic detection than the natural ruthenium isotopes which are all quadrupolar and give rise to broad resonances for arene complexes. However, ^{187}Os has a very low gyromagnetic ratio and is insensitive to detection, one of the most insensitive nuclei in the periodic table (sensitivity of detection 1.2×10^{-5} relative to ^{1}H). Hence there are relatively few reports of ^{187}Os NMR spectroscopic studies, perhaps as few as only 20 in the last 20 years.[7] In this work we show the advantage of using inverse detection methods to increase the sensitivity of ^{187}Os detection.

[a] Department of Chemistry, University of Edinburgh, West Mains Road,
Edinburgh EH9 3JJ, UK
[b] BRUKER Biospin SA
34, rue de l'industrie, 67166 Wissembourg Cedex, France
[c] Department of Chemistry, University of Warwick,
Gibbet Hill Road, Coventry CV4 7AL, UK

Results

The sandwich complexes **1** and **2** were prepared in reasonable yields as triflate salts from the appropriate dimers [(η^6-bip)(Ru/Os)Cl$_2$]$_2$ after abstraction of the chloride ligands with Ag^I triflate in acetone and further reaction of the tris-acetone complex with biphenyl in trifluoroacetic acid. Crystals of **1**·MeOH suitable for X-ray diffraction were obtained from methanol with ether infusion, and for **2** from acetonitrile with ether infusion.

X-ray Crystallography

The X-ray crystal structures of complexes **1**·MeOH and **2** are shown in Figure 1. Both exhibit the predicted bis-arene "sandwich" geometry with all six carbon atoms from both ligands involved in π-bonding to the metal. Both bound and unbound phenyl rings appear to have regular geometries, with no significant angle distortions. In both cases, the metal is positioned centrally between the two ligands, with no significant differences in metal–carbon bond

lengths between the two structures. The ruthenium complex crystallised in the monoclinic $P1\,2_1\,1$ space group and the osmium complex in the triclinic P1 space group, which results in the unit cell parameters being quite different. The propeller twist of the biphenyl ligand is significantly larger for **1** at 29.27° compared to 23.73° for **2**. The distance between the centroids of the two unbound rings also differs between the structures and is shorter for Ru complex **1** (3.486 Å) compared to Os complex **2** (3.616 Å). Crystallographic data are shown in Table 1 and selected bond lengths and angles are listed in Table 2.

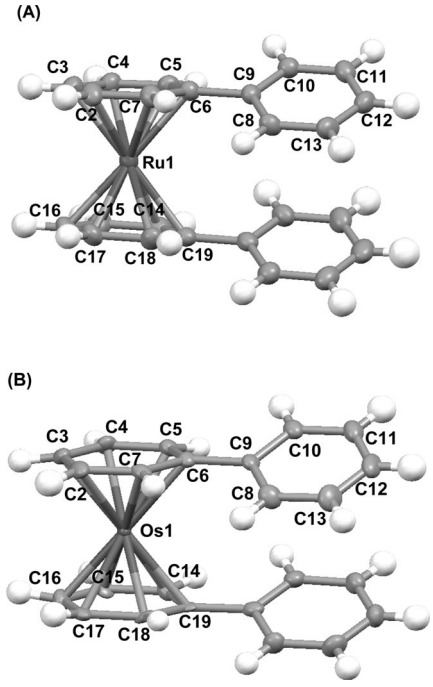

Figure 1. X-ray crystal structures and atomic numbering schemes for cations of (A) $[Ru(\eta^6\text{-bip})_2](OTf)_2\cdot MeOH$ (**1**·MeOH) and (B) $[Os(\eta^6\text{-bip})_2](OTf)_2$ (**2**). Thermal ellipsoids at 50% probability level.

Table 1. Crystallographic data and solution refinements for $[Ru(\eta^6\text{-bip})_2](OTf)_2\cdot MeOH$ (**1**·MeOH) and $[Os(\eta^6\text{-bip})_2](OTf)_2$ (**2**).

	1	**2**
Formula	$C_{26}H_{20}F_6RuO_6S_2$	$C_{26}H_{20}F_6O_6OsS_2$
[M]	707.08	796.76
Colour	yellow	colourless
Crystal system	monoclinic	triclinic
Crystal size [mm]	$0.64\times0.53\times0.44$	$0.44\times0.39\times0.23$
Space group	$P1\ 2_1\ 1$	$P1$
a [Å]	13.3276(5)	12.0707(3)
b [Å]	16.0939(6)	13.6782(3)
c [Å]	14.0367(5)	14.6938(3)
α [°]	90	113.2370(10)
β [°]	110.281(2)	94.8610(10)
γ [°]	90	115.5100(10)
U [Å^3]	2824.12(18)	1914.70(8)
Z	4	3
D_c [mg M^{-3}]	1.740	2.073
$F(000)$	1488	1158
Goodness of fit on F^2	0.9867	0.8746
Conventional R	0.0410	0.0321
Weighted R	0.1121	0.0957

Table 2. Selected bond lengths [Å] and angles [°] for $[Ru(\eta^6\text{-bip})_2](OTf)_2\cdot MeOH$ (**1**·MeOH) and $[Os(\eta^6\text{-bip}_2)](OTf)_2$ (**2**).

Bond/angle	**1** (Ru)	**2** (Os)
M(1)–C(2)	2.226(4)	2.239(5)
M(1)–C(3)	2.208(4)	2.229(5)
M(1)–C(4)	2.209(4)	2.223(5)
M(1)–C(5)	2.221(4)	2.227(5)
M(1)–C(6)	2.268(4)	2.274(5)
M(1)–C(7)	2.229(4)	2.214(6)
M(1)–C(14)	2.224(4)	2.237(5)
M(1)–C(15)	2.202(4)	2.215(6)
M(1)–C(16)	2.210(4)	2.214(5)
M(1)–C(17)	2.204(4)	2.227(5)
M(1)–C(18)	2.222(4)	2.231(5)
M(1)–C(19)	2.279(4)	2.290(5)
C(2)–C(3)–C(4)	118.3(4)	119.8(5)
C(3)–C(4)–C(5)	120.8(4)	120.8(5)
C(4)–C(5)–C(6)	120.8(4)	121.1(5)
C(5)–C(6)–C(7)	119.6(4)	117.4(5)
C(6)–C(7)–C(2)	119.5(4)	122.0(5)
C(7)–C(2)–C(3)	121.0(4)	118.9(5)
C(8)–C(9)–C(10)	120.5(4)	118.9(5)
C(9)–C(10)–C(11)	119.8(4)	120.1(5)
C(10)–C(11)–C(12)	119.9(4)	120.6(6)
C(11)–C(12)–C(13)	120.0(4)	119.7(6)
C(12)–C(13)–C(8)	121.4(4)	120.6(6)
C(13)–C(8)–C(9)	118.5(4)	120.1(6)

An interesting feature of the osmium structure is that of the three molecules present in the unit cell, two have the unbound phenyl rings of the biphenyl ligands in a staggered configuration and the other has them eclipsed. This is illustrated in Figure 2 and differs from the ruthenium structure, where all four molecules have the unbound rings in the eclipsed configuration. In solution, arene rotation is expected to be very rapid.

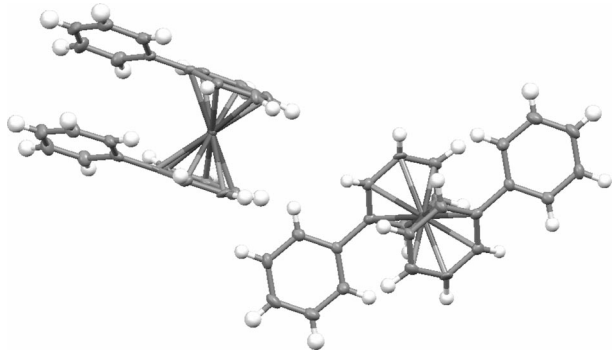

Figure 2. Diagram showing the eclipsed and staggered configurations of the biphenyl rings in $[Os(\eta^6\text{-bip})_2](OTf)_2$ (**2**).

As the complexes belong to different space groups, very different interactions and packings result within the structures. $[Ru(\eta^6\text{-bip})_2](OTf)_2$ (**1**) forms chains along the c-axis as a result of intermolecular contacts between anions and cations (Figure 3). Furthermore, two distinct intermolecular CH···π interactions of 2.877 and 3.089 Å exist between pairs of cations (Figure 4).

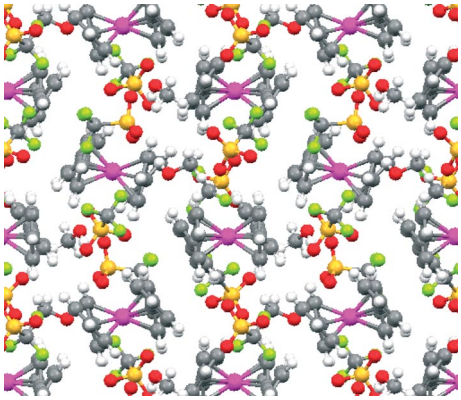

Figure 3. Crystal packing observed along the *c*-axis for $[Ru(\eta^6\text{-bip})_2](OTf)_2$·MeOH (**1**·MeOH). Intermolecular contacts between anions and cations lead to the formation of chains through the structure.

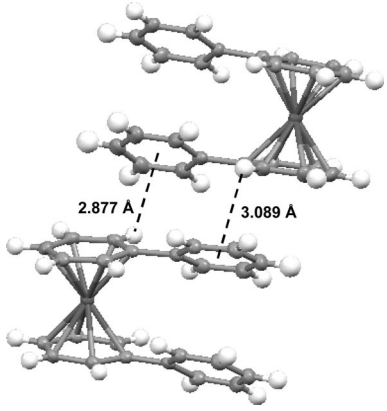

Figure 4. Intermolecular CH···π interactions (involving CH groups C114–H1141 and C18–H181) between pairs of cations in the X-ray structure of $[Ru(\eta^6\text{-biph}_2)](OTf)_2$·MeOH (**1**·MeOH).

Contrastingly, $[Os(\eta^6\text{-bip})_2](OTf)_2$ (**2**) displays chains of alternating eclipsed and staggered metal cations with intermolecular CH···π interactions of 3.037 Å between the two forms (Figure 5). Perpendicular to this, chains of eclipsed cations also exist as a result of both inter- and intramolecular π–π stacking with angle offsets and distances of 12.37° and 3.309 Å and 21.38° and 3.616 Å, respectively (Figure 6).

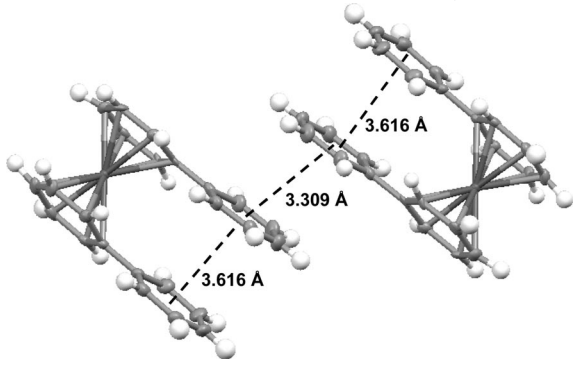

Figure 6. Intra- and intermolecular π–π stacking between eclipsed cations in the X-ray structure of $[Os(\eta^6\text{-bip})_2](OTf)_2$ (**2**).

$^1H/^{187}Os$ Heteronuclear Multiple Bond Correlation (HMBC) Spectroscopy

In addition to one-dimensional NMR spectroscopic characterisation of $[Os(\eta^6\text{-bip})_2](OTf)_2$ (**2**), it was possible to observe proton-osmium correlations for this complex through the use of $^1H/^{187}Os$ HMBC spectroscopy. The spectrum obtained is shown in Figure 7. The ^{187}Os signal is seen to couple to all the ^1H signals except for that at ca.

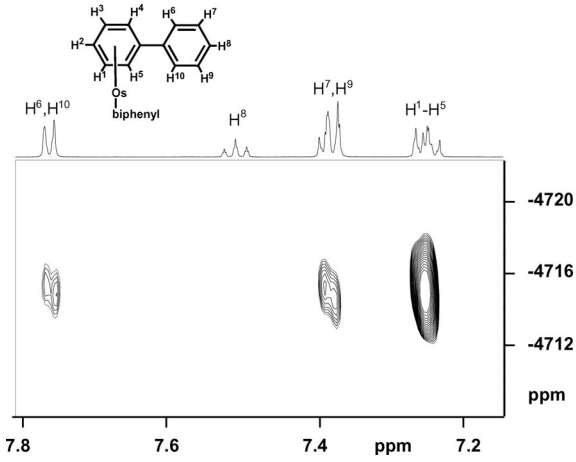

Figure 7. $^1H/^{187}Os$ HMBC spectrum of a 25 mM solution of $[Os(\eta^6\text{-bip})_2](OTf)_2$ (**2**) in d_4-MeOD at 500 MHz (^1H). Peak labels correspond to the structure shown, where both biphenyl ligands are equivalent.

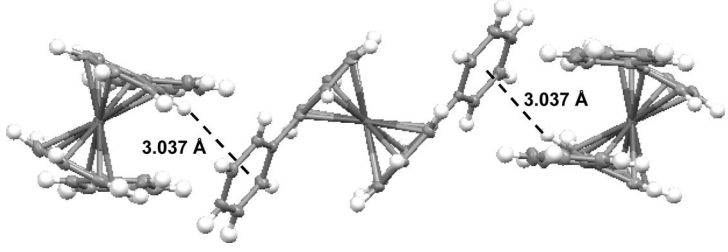

Figure 5. Intermolecular CH···π interactions between eclipsed and staggered cations in the X-ray structure of $[Os(\eta^6\text{-bip}_2)](OTf)_2$ (**2**).

7.52 ppm, which corresponds to the *para*-protons on the unbound biphenyl rings at the furthest distance from the osmium centre.

Discussion

$^{1}H/^{187}Os$ Heteronuclear Multiple Bond Correlation (HMBC) Spectroscopy

Osmium has two magnetically-active nuclei, ^{187}Os and ^{189}Os, although the latter is not used in NMR spectroscopic techniques as it has spin $^{3}/_{2}$ and a large quadrupole moment. ^{187}Os has spin 1/2 and is therefore much more useful, however its low natural abundance of 1.64% and very low gyromagnetic ratio, render it one of the most insensitive nuclei in the periodic Table and therefore its detection by conventional one-dimensional NMR spectroscopy is challenging. It is, however, possible to observe it indirectly using X-{^{187}Os} two dimensional NMR spectroscopy (X = ^{1}H or ^{31}P).[8,9] Such inverse detection techniques can increase sensitivity by over 10000 fold, although examples in the literature are much less common than for other transition metals.[7] A further challenge is that the chemical shift range for ^{187}Os is very large.[10] The most common reference material is osmium tetroxide (OsO_4).

The closest related complexes to $[Os(\eta^6\text{-biphenyl})_2](OTf)_2$ (**2**) which have been studied are mono-arene complexes of osmium, where the chemical shift of the ^{187}Os signal has been found to be highly sensitive to both its chemical and steric environments.[7] The osmium signal for **2** at ca.–4715 ppm is shifted significantly from the average position obtained for mono-arene complexes (with e.g. a monodentate phosphane or phosphite ligand and two halido ligands) of ca. –3000 ppm[7,11,12] as a result of the increased shielding provided by the second arene ligand. As the first proton-osmium correlation observed for a bis-arene complex, this result is highly significant, giving new insight into the electronic effect that the ligands have on the central metal atom in such structures.

X-ray Crystallography

There are very few examples of structures of osmium bis-arene complexes in the literature therefore that of $[Os(\eta^6\text{-bip})_2](OTf)_2$ (**2**) provides a valuable addition to these.[13,14] Known structures containing biphenyl are restricted to mono-arene complexes,[15] where the average $metal\text{-}arene_{centroid}$ bond length of 1.636 Å is much shorter that that observed here (1.727 Å). This is a result of **2** possessing two η^6-coordinated arenes which compete for the π–electron density, thus weakening and lengthening the bonds. The close similarity in structure to the ruthenium analogue $[Ru(\eta^6\text{-bip})_2](OTf)_2$ (**1**), follows trends observed for a number of mono-arene complexes of the two metals.[15,16] A previous determination of the structure of the $[Ru(\eta^6\text{-bip})_2]^{2+}$ cation was reported in 1995 by Porter et al.[17] and although bond lengths and angles are not significantly different, the use of different counterions renders **1** with a unique structure. The different space groups and packing motifs observed for **1** and **2** may be, in part, due to the use of different solvents during the crystallisation process (methanol cf. acetonitrile). Four molecules of methanol are incorporated into the unit cell of the former, each of which possesses a short O(H) contact with a CH group of the unbound phenyl ring of the ruthenium cation. In contrast, no acetonitrile was found in crystals of the osmium complex.

Both crystal structures possess CH/π and π–π stacking interactions. The phenomenon of CH/π interactions is quite well documented and has received interest due to their ability to play important roles in protein stability and in recognition processes.[18] Such interactions range from weak (CH···π center 2.6–3.0 Å) to very strong (CH···π center < 2.6 Å),[19] hence those observed here for $[Ru(\eta^6\text{-bip})_2](OTf)_2$ (**1**) and $[Os(\eta^6\text{-bip})_2](OTf)_2$ (**2**) of between ca. 2.9 and 3.1 Å can be classified as weak. Facial π–π interactions are also very important in nature and occur between rings with separations of between 3.3 and 3.8 Å.[20] The intramolecular π–π stacking between the unbound biphenyl rings is stronger for the ruthenium complex, with the distance between them being 0.13 Å less than for the osmium complex. This enhanced interaction may contribute to the presence of only the eclipsed conformation of the rings in **1** compared to both eclipsed and staggered conformations for **2**.

Experimental Section

Syntheses

$[Ru(\eta^6\text{-bip})_2](OTf)_2$ (1): $[(\eta^6\text{-bip})RuCl_2]_2$[15] (0.20 g, 0.33 mmol) was stirred with AgOTf (0.36 g, 1.32 mmol) in dry acetone (9 mL) for 1 h at ambient temperature, under argon. Filtration of the AgCl precipitate yielded a clear red solution which was centrifuged for 10 min. Excess solvent was removed in vacuo, affording a red oily residue of the intermediate $[(\eta^6\text{-bip})Ru(acetone)_3](OTf)_2$. To this, biphenyl (0.12 g, 0.64 mmol) in trifluoroacetic acid (12 mL) was added and the clear, red solution stirred for 20 h at 333 K under reflux. On cooling, the red solution became cloudy, with precipitation of a light yellow powder. Further precipitation occurred on addition of diethyl ether and the product was filtered, washed with diethyl ether and dried in vacuo prior to analysis (Yield: 235 mg, 52.0%). $C_{26}H_{20}F_6O_6RuS_2$ (707.62): calcd. C 44.13, H 2.85; found C 43.97, H 2.58. ESI MS: calcd. for $RuC_{24}H_{20}^{2+}$ $[M - 2OTf]^{2+}$ *m*/*z* 205.03; found 205.10. ^{1}H NMR (500 MHz, D_2O): δ = 7.02 (t, 2 H, bound Ph), 7.11 (t, 4 H, bound Ph), 7.24 (t, 4 H, unbound Ph), 7.31 (d, 4 H, bound Ph), 7.41 (d, 4 H, unbound Ph), 7.54 (t, 2 H, unbound Ph) ppm.

Yellow block crystals of **1**·MeOH suitable for X-ray diffraction were obtained by slow diffusion of gaseous diethyl ether into a methanol solution of the complex at 298 K.

$[Os(\eta^6\text{-bip})_2](OTf)_2$ (2): $[(\eta^6\text{-bip})OsCl_2]_2$[15] (0.26 g, 0.31 mmol) was stirred with AgOTf (0.32 g, 1.25 mmol) in dry acetone (9 mL) for 1 h at ambient temperature, under argon. Filtration of the AgCl precipitate yielded a clear orange solution which was then centrifuged for 10 min to ensure no solid remained suspended in solution. Excess solvent was removed in vacuo, affording an orange oil of the intermediate $[(\eta^6\text{-bip})Os(acetone)_3](OTf)_2$. Biphenyl (0.10 g,

0.62 mmol) in trifluoroacetic acid (10 mL) was added to the [(η^6-bip)Os(acetone)$_3$](OTf)$_2$ and the cloudy, orange solution stirred for 20 h at 333 K. After cooling, addition of diethyl ether resulted in precipitation of a pale grey powder. This was filtered, washed several times with diethyl ether and dried in vacuo prior to analysis (Yield: 236 mg, 47.8%). Colourless plate crystals of **2** suitable for X-ray diffraction were obtained by diffusion of diethyl ether into an acetonitrile solution of the complex at 277 K. $C_{26}H_{20}F_6O_6OsS_2$ (796.78): calcd. C 39.19, H 2.53; found C 38.93, H 2.29. ESI MS: calcd. for $OsC_{24}H_{20}^{2+}$ [M – 2OTf]$^{2+}$ *m*/*z* 250.06, found 250.08. ^{1}H NMR (500 MHz, D_2O): δ = 7.21 (m, 6 H, bound Ph), 7.26 (d, 4 H, bound Ph), 7.34 (t, 4 H, unbound Ph), 7.49 (t, 2 H, unbound Ph), 7.68 (d, 4 H, unbound Ph) ppm.

Heteronuclear Multiple Bond Correlation (HMBC) Spectroscopy: ^{1}H/^{187}Os HMBC spectroscopy was performed on a 25 mM solution of [Os(η^6-bip)$_2$](OTf)$_2$ (**2**) in MeOD at 298 K on an Avance III 500 (^{1}H = 500.2 MHz, ^{187}Os = 11.42 MHz) spectrometer equipped with a 5 mm Triple Resonance Broadband Inverse (TBI-LR) 1H/31P/BB probe with *z*-field gradients. The 90° pulse length for osmium was 60 μs.

The osmium resonance frequency was roughly estimated from a series of 1D ^{1}H/^{187}Os HMBC experiments carried out with incremented values of the carrier frequency. In order to check for the absence of folding in the F1 dimension two gradient-enhanced HMBC spectra were recorded with different settings of the osmium spectral width, 1100 and 80 ppm. The second one, shown in Figure 7, was recorded with the following experimental conditions: 640 transients collected for each FID, 32 increments, 1/2*J* delay set to 0.1 s, recycling delay 2.25 s; three sine-shaped gradients pulses of 1 ms duration in the intensity ratio of 60:20:41.82 for coherence (echo type) selection; sine bell multiplication in both dimensions and zero filling to 128 data points in the F1 dimension was applied before Fourier transform followed by magnitude calculation. The reference frequency for the ^{187}Os chemical shift was calculated from the proton frequency of internal TMS, using a conversion factor Ξ = 2.282331.

X-ray Crystallography: Diffraction data for **1**·MeOH and **2** were collected on a Bruker (Siemens) Smart Apex CCD Diffractometer using Mo-K_α radiation equipped with an Oxford Cryosystems low-temperature device operating at 150 K. The structures were solved using direct (SHELXS-97[21] or SIR92[22]) methods and were refined against F^2 using CRYSTALS.[23] H atoms were placed in calculated positions and non-H atoms were modelled with anisotropic displacement parameters. The modelling programs Mercury 1.4 and Diamond 3.0 were used for analysis of data and generation of graphics.

CCDC-722434 (for **1**·MeOH) and -722433 (for **2**) contain the supplementary crystallographic data for this paper. These data can be obtained free of charge from The Cambridge Crystallographic Data Centre via www.ccdc.cam.ac.uk/data_request/cif.

[1] G. Jaouen, A. Vessieres, I. S. Butler, *Acc. Chem. Res.* **1993**, *26*, 361–369.

[2] A. F. A. Peacock, S. Parsons, P. J. Sadler, *J. Am. Chem. Soc.* **2007**, *129*, 3348–3357.

[3] Y. K. Yan, M. Melchart, A. Habtemariam, P. J. Sadler, *Chem. Commun.* **2005**, 4764–4776.

[4] A. Habtemariam, M. Melchart, R. Fernandez, S. Parsons, I. D. H. Oswald, A. Parkin, F. P. A. Fabbiani, J. E. Davidson, A. Dawson, R. E. Aird, D. I. Jodrell, P. J. Sadler, *J. Med. Chem.* **2006**, *49*, 6858–6868.

[5] A. F. A. Peacock, A. Habtemariam, S. A. Moggach, A. Prescimone, S. Parsons, P. J. Sadler, *Inorg. Chem.* **2007**, *46*, 4049–4059.

[6] J. C. Gray, A. Habtemariam, M. Winnig, W. Meyerhof, P. J. Sadler, *J. Biol. Inorg. Chem.* **2008**, *13*, 1111–1120.

[7] A. G. Bell, W. Kozminski, A. Linden, W. v. Philipsborn, *Organometallics* **1996**, *15*, 3124–3135.

[8] R. Benn, H. Brenneke, E. Joussen, H. Lehmkuhl, F. L. Ortiz, *Organometallics* **1990**, *9*, 756–761.

[9] M. J. Stchedroff, V. Moberg, E. Rodriguez, A. E. Aliev, J. Bottcher, J. W. Steed, E. Nordlander, M. Monari, A. J. Deeming, *Inorg. Chim. Acta* **2006**, *359*, 926–937.

[10] R. Benn, E. Joussen, H. Lehmkuhl, F. L. Ortiz, A. Rufunska, *J. Am. Chem. Soc.* **1989**, *111*, 8754–8756.

[11] J. A. Cabeza, B. E. Mann, C. Brevard, P. M. Maitlis, *J. Chem. Soc., Chem. Commun.* **1985**, 65.

[12] J. A. Cabeza, B. E. Mann, P. M. Maitlis, C. Brevard, *J. Chem. Soc., Dalton Trans.* **1988**, 629.

[13] Z. Bolin, A. Ellern, A. Sygula, R. Sygula, R. J. Angelici, *Organometallics* **2007**, *26*, 1721.

[14] M. R. J. Elsegood, P. A. Tocher, *J. Organomet. Chem.* **1990**, *391*, 239.

[15] A. F. A. Peacock, A. Habtemariam, R. Fernandez, V. Walland, F. P. A. Fabbiani, S. Parsons, R. E. Aird, D. I. Jodrell, P. J. Sadler, *J. Am. Chem. Soc.* **2006**, *128*, 1739–1748.

[16] A. F. A. Peacock, M. Melchart, R. J. Deeth, A. Habtemariam, S. Parsons, P. J. Sadler, *Chem. Eur. J.* **2007**, *13*, 2601–2613.

[17] L. C. Porter, S. Bodige, H. E. Selnau Jr., H. H. Murray III, J. M. McConnachie, *Organometallics* **1995**, *14*, 4222–4227.

[18] M. Brandl, M. S. Weiss, A. Jabs, J. Suhnel, R. Hilgenfeld, *J. Mol. Biol.* **2001**, *307*, 357.

[19] G. A. Bogdanovic, A. S.-d. Bire, S. D. Zaric, *Eur. J. Inorg. Chem.* **2002**, 1599.

[20] C. Janiak, *J. Chem. Soc., Dalton Trans.* **2000**, 3885.

[21] G. M. Sheldrick, *SHELXL-97: Program for the refinement of crystal structures*, University of Göttingen, Federal Republic of Germany, **1997**.

[22] A. Altomare, G. Cascarano, G. Giacovazzo, A. Guagliardi, M. C. Burla, *J. Appl. Crystallogr.* **1994**, *27*, 435.

[23] P. W. Betteridge, J. R. Carruthers, R. I. Cooper, K. Prout, D. J. Watkin, *J. Appl. Crystallogr.* **2003**, *36*, 1487.

Received: March 14, 2009
Published Online: May 13, 2009

